

# Sensitivity Curve Approximation using Linear Algebra

*D. Paulus*<sup>1</sup>, *V. Hong*<sup>1</sup>, *C. Idler*<sup>1</sup>, *J. Hornegger*<sup>2</sup>, *L. Csink*<sup>3</sup>

*Universität Koblenz-Landau*<sup>1</sup>  
*Computervisualistik*  
*Universitätsstr. 1*  
*56070 Koblenz, Germany*  
 paulus@uni-koblenz.de

*Lehrstuhl f. Mustererkennung*<sup>2</sup>  
*(Informatik 5), Martessstr. 3*  
*Universität Erlangen-Nürnberg*  
*91053 Erlangen, Germany*  
 joachim@hornegger.de

*Budapest Polytechnic*<sup>3</sup>  
*John von Neumann Faculty of*  
*Informatics*  
*H-1300 Budapest, Hungary*  
 csink@nik.bmf.hu

## Abstract

Calibration of color cameras requires that a calibration pattern is recorded and color responsivity curves are estimated from the recorded data. Very often, these curves are sampled at discrete wavelength, so that the calibration problem can be written as a system of linear equations. The solution of the – usually overdetermined – problem is subject to a constrained optimization problem, as these curves need to have a certain shape. In this article we apply different methods to incorporate constraints into the estimation problem while still keeping the problem linear.

## 1. Introduction

Color cameras have sensors that have unknown responsivity functions. The responsivity of typical CCD chips for red, green, and blue varies over the range of wavelengths  $\lambda$ . The sensors may even vary amongst the same type as the responsivity curves depend on the parameters of the production. Therefore, color calibration of a camera requires the estimation of color responsivity curves. If the responsivity functions are known, color pixels can be remapped to values of a standard observer. Accurate color measurements require such a mapping. In many cases, accurate color values might increase results of image analysis.

The goal is to compute these parameters auto-

matically. Usually, this is done under known illumination with a color checker and spectrometric measurements. Several unknown parameters influence the image generation process. It is usually assumed that the irradiance  $E(\lambda)$  is known. A calibration pattern<sup>1</sup> with known reflectivity  $\rho(\mathbf{x}, \lambda)$  at spatial position  $\mathbf{x}$  is recorded and color pixel vectors corresponding to the position  $\mathbf{x}$  will be used to set up an equation system for the unknown influence of the sensor (Figure 1). The function  $\rho$  models the different color patches; as we assume a Lambertian calibration pattern, the argument  $\mathbf{x}$  models the variation of the color patches and the argument  $\lambda$  accounts for the different reflectivity of the color patches with respect to the irradiation.

As the computation of the unknowns is an overdetermined system with constraints, [1] uses nonlinear optimization to compute the responsivity functions. [2] reports on several approaches and uses Fourier basis functions to approximate the responsivity curves. In the following we will derive a linear approximation of calibration parameters. We extend our theoretical approach [8] by the experimental work of [5] and adopt the notation of [4].

---

<sup>1</sup>For example the Gretag MCBeth ColorChecker, shown on the left in Figure 1

PSfrag replacements

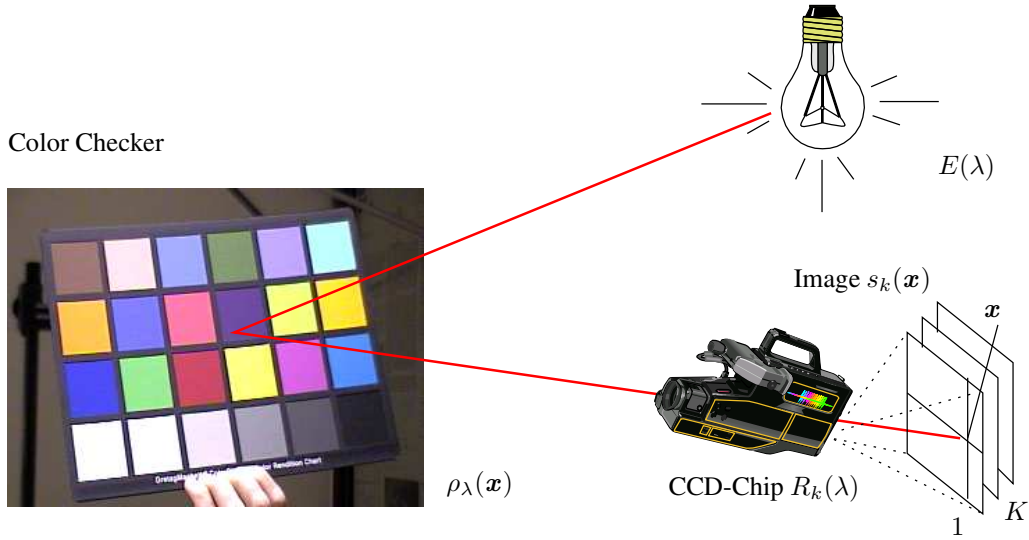


Figure 1: Sensor, reflectivity, and measurements

## 2. Device Responsivity Model

The  $K$  sensors per pixel, typically red, green, and blue for a color camera, have spectral responsivity curves  $R_k(\lambda)$ , ( $k = 1, \dots, K$ ). Any sensor channel  $k$  thereby records light intensity at position  $\mathbf{x}$  using the following energy distribution:

$$s_k(\mathbf{x}) = \int_0^\infty E(\lambda) \cdot \rho(\mathbf{x}, \lambda) \cdot R_k(\lambda) d\lambda \quad (1)$$

As noted in [1], the discrete version of (1) is often written as a sum of  $L = 31$  samples

$$s_k(\mathbf{x}) = \sum_{\lambda=1}^L E_\lambda \cdot \rho_\lambda(\mathbf{x}) \cdot R_{k,\lambda} \cdot \Delta\lambda \quad (2)$$

The vector  $\mathbf{E} = [E_\lambda]_{\lambda=1, \dots, L}$  denotes the discrete spectral energy distribution for illumination,

$$\boldsymbol{\rho}(\mathbf{x}) = [\rho_\lambda(\mathbf{x})]_{\lambda=1, \dots, L}$$

denotes the discrete spectral reflectance at position  $\mathbf{x}$ , and the matrix  $\mathbf{R} = (R_{k,\lambda})_{k=1, \dots, K, \lambda=1, \dots, L}$  denotes the discrete spectral responsivity curves of the

sensors. Using  $\Delta\lambda = 10\text{nm}$ , the whole visible range of light can be covered. In the following we discard the scalar constant  $\Delta\lambda$  in the equations for simplicity. The relation of the various variables is shown in Figure 1.

We now arrange (2) into a matrix equation, as we re-write matrix  $\mathbf{R}$  as a vector

$$\mathbf{r} = (R_{1,1} \dots R_{1,L} \dots R_{K,1} \dots R_{K,L}) \quad (3)$$

and define a  $(K \cdot N \times L \cdot K)$ -matrix  $\mathbf{C}$  consisting of either zeros or measurements  $E_\lambda \rho_\lambda^{(i)}$  at  $i = 1, \dots, N$  points  $E_\lambda \rho_\lambda^{(i)}$  to get

$$\mathbf{s} = \mathbf{C} \mathbf{r} \quad (4)$$

More specifically, with  $K = 3$  for red, green and

blue we get

$$\begin{pmatrix} s_{\text{red},1} \\ s_{\text{green},1} \\ s_{\text{blue},1} \\ \dots \\ s_{\text{red},N} \\ s_{\text{green},N} \\ s_{\text{blue},N} \end{pmatrix} = \mathbf{C} \begin{pmatrix} R_{\text{red},1} \\ R_{\text{red},2} \\ \vdots \\ R_{\text{red},L} \\ \dots \\ R_{\text{blue},1} \\ R_{\text{blue},2} \\ \vdots \\ R_{\text{blue},L} \end{pmatrix} \quad (5)$$

and the matrix  $\mathbf{C}$  is shown below in (6).

Assuming that we have standard illumination, i.e.,  $\mathbf{E}_\lambda$  is known, and knowledge on the reflectivity and surface of the object, i.e.,  $\rho_\lambda$  are known, we can measure  $\mathbf{s}$  and compute the unknown vector  $\mathbf{r}$ . Correspondence of known colors and their position in the image accounts for the positions  $\mathbf{x}$  in (2) and for the  $N$  measurement points in (5). In order to get a solution of the set of linear equations, the number of measurements  $N$  must be greater than  $L$ .

The solution of (4) for the unknowns in  $\mathbf{r}$  requires regularization [1]. The following criteria 1-4 are used in [1]:

1. sensor positivity:  
 $R_{k,\lambda} \geq 0$  where  $k \in \{1, \dots, K\}$  and  $\lambda \in \{1, \dots, L\}$
2. sensor smoothness:  
 $|R_{k,\lambda} - R_{k,\lambda+1}| < T$  for some threshold  $T$  and  $\lambda \in \{1, \dots, L-1\}$
3. unimodality:  
 $\forall k \exists \kappa : R_{k,\lambda} < R_{k,\lambda+1}$  for  $\lambda \leq \kappa$  and  $R_{k,\lambda} > R_{k,\lambda+1}$  for  $\lambda > \kappa$
4. bounded prediction error:  
 $|s_i - \sum_{j=1}^L C_{i,j} \cdot r_j| \leq \epsilon$  for  $i \in \{1, \dots, N\}$
5. rank constraint:  
 $\text{rank}(\mathbf{C}) \in \{6, 7, 8\}$ .

To obtain a subset of constraints 1-4, several optimization techniques have been proposed, such as linear programming or quadratic programming [1].

The rank constraint has been tested empirically for three color channels ( $K = 3$ ) in [6, 7].

Of course, (1) assumes a linear relation of image intensity and sensor response which needs to be computed from real data by reverting the gamma correction of the camera.

### 3. Simultaneous Optimization

In the following we derive an optimization of the criteria 1-5 where some of the criteria 1-4 have to be replaced by slightly weaker constraints. Instead of iterative optimization techniques, slightly weaker constraints lead to a linear problem that will be solved using singular value decomposition (SVD). Inequalities are replaced by a single objective function which has to be minimized finally. For each of the criteria we introduce a term in the objective function.

Clearly, the criterion 4 is described by

$$\|\mathbf{C}\mathbf{r} - \mathbf{s}\|^2 \rightarrow \min \quad . \quad (7)$$

Constraint 2 for sensor smoothness requires that two adjacent coefficients  $R_{k,\lambda}$ ,  $R_{k,\lambda+1}$  differ only up to a threshold. This constraint is slightly weakened as we use

$$\sum_{k=1}^K \sum_{\lambda=1}^{L-1} (R_{k,\lambda} - R_{k,\lambda+1})^2 \rightarrow \min \quad . \quad (8)$$

Since the squared difference is used instead of the norm  $|R_{k,\lambda} - R_{k,\lambda+1}|$  as in constraint 2, large differences are more penalized and imply a bias. We define a  $(N \times K)$  auxiliary matrix

$$\tilde{\mathbf{D}} = \begin{pmatrix} 1 & 0 & 0 & 0 & \dots & \dots & 0 \\ -1 & 2 & -1 & 0 & \dots & \dots & 0 \\ 0 & -1 & 2 & -1 & 0 & \dots & 0 \\ \dots & & & & & & \\ 0 & \dots & 0 & -1 & 2 & -1 & 0 \\ 0 & \dots & \dots & 0 & -1 & 2 & -1 \\ 0 & \dots & \dots & \dots & 0 & 0 & 1 \end{pmatrix} .$$

$$\mathbf{C} = \begin{pmatrix} E_1 \rho_1^{(1)} & \cdots & E_L \rho_L^{(1)} & 0 & \cdots & 0 & 0 & \cdots & 0 \\ 0 & \cdots & 0 & E_1 \rho_1^{(1)} & \cdots & E_L \rho_L^{(1)} & 0 & \cdots & 0 \\ 0 & \cdots & 0 & 0 & \cdots & 0 & E_1 \rho_1^{(1)} & \cdots & E_L \rho_L^{(1)} \\ \vdots & \vdots \\ E_1 \rho_1^{(N)} & \cdots & E_L \rho_L^{(N)} & 0 & \cdots & 0 & 0 & \cdots & 0 \\ 0 & \cdots & 0 & E_1 \rho_1^{(N)} & \cdots & E_L \rho_L^{(N)} & 0 & \cdots & 0 \\ 0 & \cdots & 0 & 0 & \cdots & 0 & E_1 \rho_1^{(N)} & \cdots & E_L \rho_L^{(N)} \end{pmatrix} \quad (6)$$

and another  $(K \cdot L \times K \cdot L)$  matrix

$$\mathbf{D} = \begin{pmatrix} \tilde{\mathbf{D}} & \mathbf{0} & \cdots & \mathbf{0} \\ \mathbf{0} & \tilde{\mathbf{D}} & \cdots & \mathbf{0} \\ \vdots & \vdots & \vdots & \vdots \\ \mathbf{0} & \mathbf{0} & \mathbf{0} & \tilde{\mathbf{D}} \end{pmatrix} .$$

Then, constraint 2 can be expressed as

$$\sum_{k=1}^K \sum_{\lambda=1}^{L-1} (R_{k,\lambda} - R_{k,\lambda+1})^2 \rightarrow \min \quad (9)$$

which, using (3) is equivalent to

$$\mathbf{r}^T \mathbf{D} \mathbf{r} \rightarrow \min \quad (10)$$

The derivatives are

$$\frac{\partial}{\partial \mathbf{r}} \mathbf{r}^T \mathbf{D} \mathbf{r} = 2 \cdot \mathbf{r}^T \mathbf{D} \quad (11)$$

as  $\mathbf{D}$  is symmetric. Combining (10) and (7) we get

$$f := \|\mathbf{C} \mathbf{r} - \mathbf{s}\|^2 + \mu \|\mathbf{r}^T \mathbf{D} \mathbf{r}\| \rightarrow \min \quad (12)$$

for a fixed  $\mu > 0$ . Computing the derivatives of (12) we get

$$\frac{\partial f}{\partial \mathbf{r}} = 2 \mathbf{r}^T \mathbf{C}^T \mathbf{C} - 2 \mathbf{s}^T \mathbf{C} + 2 \mu \cdot \mathbf{r}^T \mathbf{D} \quad (13)$$

which is a row vector of dimension  $K \cdot L$ . We set

$$\frac{\partial f}{\partial \mathbf{r}} = 0$$

and solve that for  $\mathbf{r}$ . Thus we get

$$\mathbf{r}^T (\mathbf{C}^T \mathbf{C} + \mu \cdot \mathbf{D}) = \mathbf{s}^T \mathbf{C} \quad (14)$$

As  $(\mathbf{C}^T \mathbf{C} + \mu \cdot \mathbf{D})$  is symmetric and positive definite, we get

$$\mathbf{r} = (\mathbf{C}^T \mathbf{C} + \mu \cdot \mathbf{D})^{-1} \mathbf{C}^T \mathbf{s} \quad (15)$$

This regularization is similar, but not identical with the Tikhonov regularization used in [9].

We now turn to the rank constraint 5. To enforce this, we factorize

$$\mathbf{C} = \mathbf{U} \mathbf{\Sigma} \mathbf{V}^T$$

using singular value decomposition, i.e.  $\mathbf{\Sigma}$  is the diagonal matrix containing the singular values  $\sigma_i$  of  $\mathbf{C}$ ,  $\mathbf{\Sigma} = \text{diag}(\sigma_i)$  with  $\sigma_i \geq \sigma_{i+1}$ . It is well known from linear algebra that setting singular values to 0 in  $\mathbf{\Sigma}$  yielding  $\mathbf{\Sigma}'$  we can enforce the rank of  $\mathbf{U} \mathbf{\Sigma}' \mathbf{V}^T$ .

We introduce a matrix

$$\mathbf{P} = [P_{ij}]_{i,j=1,\dots,N}$$

where  $P_{ij} = 1$  for the first eight elements on the diagonal and 0 everywhere else; this matrix is used to generate  $\mathbf{\Sigma}'$  as

$$\mathbf{\Sigma}' = \mathbf{P} \mathbf{\Sigma} .$$

We check  $P_{9,9} = \sigma_9 > \theta$  for some small threshold  $\theta$ ; if this is not true, our measurement matrix  $\mathbf{C}$  cannot be correct or it contains too much measurement noise. Integrating this into (15) gives the new combined equation

$$\mathbf{r} = (\mathbf{V} \mathbf{\Sigma}' \mathbf{\Sigma} \mathbf{V}^T + \mu \cdot \mathbf{D})^{-1} \mathbf{V} \mathbf{\Sigma}' \mathbf{U}^T \mathbf{s} \quad (16)$$

We now need to check whether the positivity of the results is valid. If not, we discard the result.

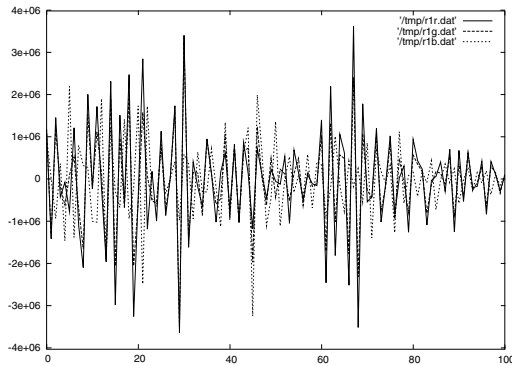


Figure 2: Solution with  $\mu = 0$ , i.e. by pseudo inverse

#### 4. Experiments

In [3], data are shown for  $K = 3$  and  $L = 101$ .<sup>2</sup> We used these samples in our experiments. As can be seen from Figure 2, regularization is required.

[2] used various basis functions such as a Fourier basis to approximate the responsivity curves by a linear combination of these functions. Thereby unimodality of the responsivity curves can be achieved. A solution of (17) without further constraints will yield a solution, that may have local maxima, but other than that is feasible.

It turned out in the experiments that enforcing the rank to 8 in (16) leads to a matrix with a large condition number. The rank was thus enforced as in

$$r = (V \Sigma^2 V^T + \mu \cdot D)^{-1} V \Sigma' U^T s \quad (17)$$

which lead to mathematically more stable results. Dark current has been subtracted from the sample values and outliers have been ignored.

Forcing the rank of  $C$  to 25 by (17) results in curves that are similar to those of the full rank  $C$ , which numerically is 303 (Figure 3). Thereby, many operations can be saved in the computation. On the other hand, strong rank enforcement will not always yield better results, as it can be seen in Figure 4. In our experiments, reduction of the numerical rank

<sup>2</sup>The data are available on the internet in [http://www.cs.berkeley.edu/~kobus/research/data/camera\\_calibration/index.html](http://www.cs.berkeley.edu/~kobus/research/data/camera_calibration/index.html).

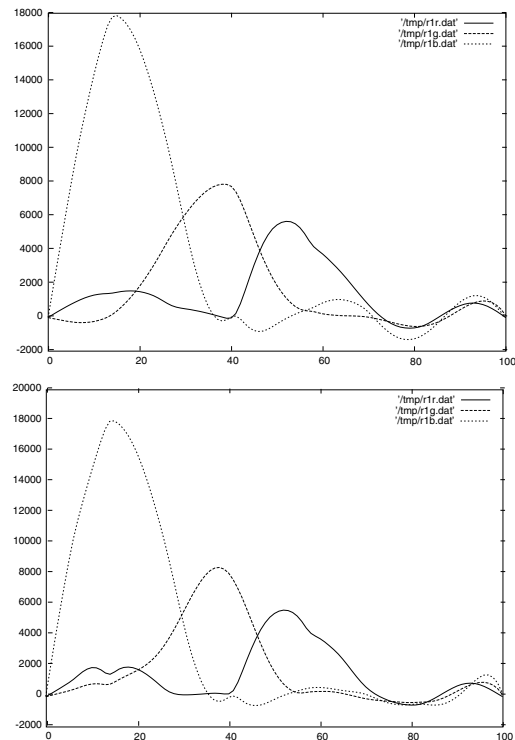


Figure 3: Solutions for  $\mu = 0.001$  rank enforced to 25 by (17) (top), and without rank constraint (bottom)

by 20 to approximately 280 gave much better results than a reduction to rank 8 which results in too much smoothing of the curves.

#### 5. Conclusion

The high degree of similarity to the results of [2] (Figure 4) justifies this linear approach. From the figures it is clear that the positivity constraint can be fulfilled automatically by the smoothness regularization, if  $\mu < 0.01$  with additional clipping. Unimodality is not obtained without additional constraints or tools. In practice, it can be enforced by clipping the curves to zero when they reach a local minimum. This is also possible, if  $\mu > 0.01$  is chosen and negative values are computed for the three curves.

As we have derived a complete closed-form so-

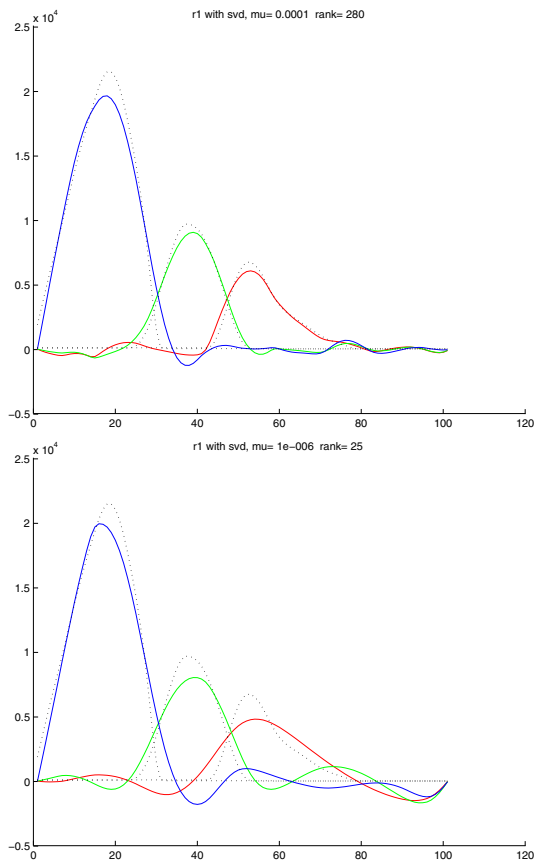


Figure 4: Solutions for  $\mu = 0.0001$  rank reduced by 23 to 280 (top) and rank enforced to 23 with  $\mu = 0.00001$  (bottom). The dotted lines show results of [2].

lution of the problem, further parameters can be integrated easily into the equations, such as e.g. spatially varying reflectivity functions.

## References

- [1] A. Alsam and G. Finlayson. Recovering spectral sensitivities with uncertainty. In *Proceedings of the First international Conference CGIV*, pages 22–26, Poitiers, France, 2002.
- [2] K. Barnard and B. Funt. Camera characterization for color research. *Color Research and Application*, 27(3):153–164, 2002.
- [3] K. Barnard, L. Martin, B. Funt, and A. Coath. A data set for color research. *Color Research and Application*, 27(3):148–152, 2002.
- [4] H. Haußecker. Interaction of radiation with matter. In B. Jähne, P. Geißler, and H. Haußecker, editors, *Handbook of Computer Vision and Applications*, volume 1, pages 37–63. Academic Press, San Diego, 1999.
- [5] C. Idler. Schätzung spektraler Sensitivitätskurven, 2003. Student’s thesis, Computervisualistik AGAS, Universität Koblenz-Landau.
- [6] L.T. Maloney. Evaluation of linear models of surface spectral reflectance with small numbers of parameters. *J. Opt. Soc. Am. A*, 3:1673–1683, 1986.
- [7] J. P. S. Parkkinen, J. Hallikainen, and T. Jaaskelainen. Characteristic spectra of munsell colors. *J. Opt. Soc. Am. A*, 6:318–322, 1989.
- [8] D. Paulus, J. Hornegger, and L. Csink. Linear approximation of sensitivity curve calibration. In K.-H. Franke, editor, *8. Workshop Farb-bildverarbeitung*, pages 3–10, Ilmenau, 2002. Schriftenreihe des Zentrums für Bild- und Signalverarbeitung e.V. Ilmenau, 1/2002.
- [9] Piana and J.C. Brown. Optimal inversion of hard x-ray bremsstrahlung spectra. *Astron. Astrophys. Suppl.*, 132:291–299, 1998.